ChemPubSoc Europe

DOI: 10.1002/cssc.201600333

CHEMSUSCHEM Full Papers

Stable Deep Doping of Vapor-Phase Polymerized Poly(3,4-ethylenedioxythiophene)/Ionic Liquid Supercapacitors

Christoffer Karlsson,*[a] James Nicholas,[b, c] Drew Evans,[b] Maria Forsyth,[d] Maria Strømme,[a] Martin Sjödin,[a] Patrick C. Howlett,[d] and Cristina Pozo-Gonzalo*[d]

Liquid-solution polymerization and vapor-phase polymerization (VPP) have been used to manufacture a series of chloride- and tosylate-doped poly(3,4-ethylenedioxythiophene) (PEDOT) carbon paper electrodes. The electrochemistry, specific capacitance, and specific charge were determined for single electrodes in 1-ethyl-3-methylimidazolium dicyanamide (emim dca) ionic liquid electrolyte. VPP-PEDOT exhibits outstanding properties with a specific capacitance higher than 300 $F g^{-1}$, the highest value reported for a PEDOT-based conducting polymer, and doping levels as high as 0.7 charges per monomer were achieved. Furthermore, symmetric PEDOT supercapacitor cells with the emim dca electrolyte exhibited a high specific capacitance (76.4 $F g^{-1}$) and high specific energy (19.8 $Wh kg^{-1}$). A Ragone plot shows that the VPP-PEDOT cells combine the high specific power of conventional ("pure") capacitors with the high specific energy of batteries, a highly sought-after target for energy storage.

Introduction

Conducting polymers have been the focus of research for more than 30 years as they have a wide range of applications such as energy storage, solar cells, actuators, and electrochromic displays.[1] They offer many advantages such as low-temperature manufacturing methods from inexpensive and sustainable resources and the possibility to realize flexible devices.[1c,2] Energy-storage devices based on conducting polymers bridge the gap between capacitors and batteries in terms of power and energy capabilities, which means that they can be electrochemically cycled faster than batteries and can store more energy than pure capacitors.[2b,3] The use of conducting polymers as the active charge-carrying component in supercapacitor devices has been reviewed extensively.[1c,2a,4] Research in this area focuses mostly on the increase of the available specific charge, energy, and power, for example, by synthesizing nanostructured and composite materials,[5] by investigating the influence of the electrolyte,[6] and so on.[4] Among conducting polymers, poly(3,4-ethylenedioxythiophene) (PEDOT) is a good candidate for supercapacitors because of its high chemical and electrochemical stability in comparison with other conducting polymers. However, PEDOT presents a low theoretical specific capacitance of 210 $F g^{-1}$ (if we assume a potential window of 1.2 V) because of the low doping level and high molar mass.[1c,7] Attempts to increase the specific capacitance have been pursued mostly by the structural modification of PEDOT.[8] A sponge-like PEDOT structure synthesized by ultrasonic irradiation (100 $F g^{-1}$),[9] the selective fabrication of PEDOT nanocapsules and mesocellular foams (155 and 170 $F g^{-1}$, respectively),[10] and PEDOT nanotubes (140 $F g^{-1}$)[11] are some examples.

Vapor-phase polymerization (VPP) has been used to polymerize PEDOT for use in a range of energy-related devices based on thermoelectric energy harvesting,[12] batteries,[13] and capacitors.[5d,14] The polymerization process itself relies on the condensation of the monomer vapor onto a liquid film that contains an Fe^{3+} salt.[15] The Fe^{3+} acts as the oxidant and is subsequently removed during washing, and the associated anions remain within the PEDOT structure to act as the dopant. This doping is essential for the creation and stabilization of the positive charge carriers along the conjugated backbone of the PEDOT. The doping level itself is responsible for the changes in the electronic and optical properties of PEDOT.[12b] If the PEDOT is then placed in an electrolyte, the doping level can be modified electrochemically. This allows the PEDOT to store or expel cations/anions, which depends on

[a] Dr. C. Karlsson, Prof. M. Strømme, Prof. M. Sjödin
Nanotechnology and Functional Materials
Department of Engineering Sciences
The Ångström Laboratory
Uppsala University
Box 534, SE-751 21 Uppsala (Sweden)
E-mail: Christoffer.Karlsson@Angstrom.uu.se

[b] J. Nicholas, Prof. D. Evans
Thin Film Coatings Group, Future Industries Institute
University of South Australia
Adelaide, South Australia, 5001 (Australia)

[c] J. Nicholas
Department of Chemistry
University of Bath
Bath, BA2 7AY (United Kingdom)

[d] Prof. M. Forsyth, Prof. P. C. Howlett, Dr. C. Pozo-Gonzalo
ARC Centre of Excellence for Electromaterials Science
Deakin University
Burwood, 3125 (Australia)
E-mail: cristina.pozo@deakin.edu.au

Supporting Information and the ORCID identification number(s) for the author(s) of this article can be found under http://dx.doi.org/10.1002/cssc.201600333.

whether the PEDOT is reduced or oxidized. It is this ability to reduce and oxidize easily and reproducibly that makes PEDOT an attractive conducting polymer material for use in supercapacitors. As an example, Kaner and co-workers utilized VPP-PEDOT doped with Cl^- to generate symmetric capacitor cells that had a specific power and specific energy of 3500 W kg^{-1} and 2.2 Wh kg^{-1}, respectively, and a specific capacity of 175 F g^{-1}.[5d] Beyond doped PEDOT, the VPP process affords the opportunity to incorporate other materials within the film. For example, polymers, triblock copolymers, and 2D nanomaterials can be embedded within the polymer thin film to lead to enhanced properties such as electrical conductivity, mechanical strength, and electrocatalytic efficiency.[5b,16]

Although most supercapacitor research has been focused on either aqueous or conventional organic media as the electrolyte, ionic liquids are an alternative and promising type of electrolyte that have received widespread attention as electrolytes in energy-storage devices, which include batteries, fuel cells, thermo-electrochemical cells, dye-sensitized solar cells, and supercapacitors, because of their outstanding properties.[17] Ionic liquids are composed entirely of ions and they are in the liquid phase below 100 °C. They offer many advantages as electrolytes such as chemical and electrochemical stability, low flammability, ionic conductivity, and negligible vapor pressure, which depends on the cation–anion combination.[17a] Importantly, the enhanced electrochemical stability offered by ionic liquid electrolytes in a supercapacitor device can be translated into an increase of the accessible energy density of the device.

Of relevance to the current work is the recent report of an ionic liquid electrolyte shown to support the reversible deposition and dissolution of Zn for reversible Zn batteries.[18] Simons et al. studied two different dicyanamide-based ionic liquids, 1-ethyl-3-methylimidazolium dicyanamide (emim dca) and *N*-butyl-*N*-methylpyrrolidinium dicyanamide, as electrolytes to support the Zn^{2+}/Zn^0 electrochemistry.[19] The imidazolium-based ionic liquid, emim dca, showed the most favorable properties for the deposition and stripping of Zn metal. As a result of the abovementioned promising results of conducting polymers in energy-storage devices, we also reported the validity of a Zn/PEDOT battery using emim dca as the electrolyte, which showed high efficiency and cycling ability and performed over 320 cycles with no indication of a short circuit. Both the Zn and PEDOT surfaces showed minimal signs of degradation.[6b]

The use of conducting polymers as the active material in energy-storage devices is challenging because of several issues, which include poor stability and low specific charge and capacitance.[1i,20] In particular, the low practical specific charge and capacitance are related to the doping level, which needs to be limited to low values to achieve an acceptable stability.[1i,20,21] Therefore, the search for conditions under which conducting polymers can be charged to high doping levels without overoxidation and degradation is an attractive target. This has motivated the present study of the performance of PEDOT as electroactive material in supercapacitors cells with the emim dca electrolyte.

Although polythiophene and its derivatives have been synthesized and characterized in various ionic liquids previously, both for energy storage and other applications, emim dca had not been investigated before our recent study of Zn/PEDOT hybrid capacitor cells.[6b] Therefore, in the present study, we report the electrochemistry of a series of PEDOT electrodes in emim dca electrolyte, as well as the performance of symmetric capacitor cells. We employ PEDOT synthesized from liquid solution with two different oxidants, as well as VPP-PEDOT with an added triblock copolymer (vide infra), and discuss the similarities and differences with respect to the polymerization conditions.

Results

PEDOT samples

SEM micrographs of the different PEDOT materials are shown in Figure 1. Chloride- and tosylate-doped PEDOT (PEDOT-Cl and PEDOT-OTs, respectively) exhibited the "cauliflower" morphology that is typical for conducting polymers synthesized from liquid solution.[22,23] Both types of PEDOT formed a uniform coating on the carbon paper substrate with limited penetration through the bulk of the substrate. Only 5% binder and no conducting additive was used in the coating mixture, and an increase of the amount of binder (up to 50%) did not improve the adhesion further.

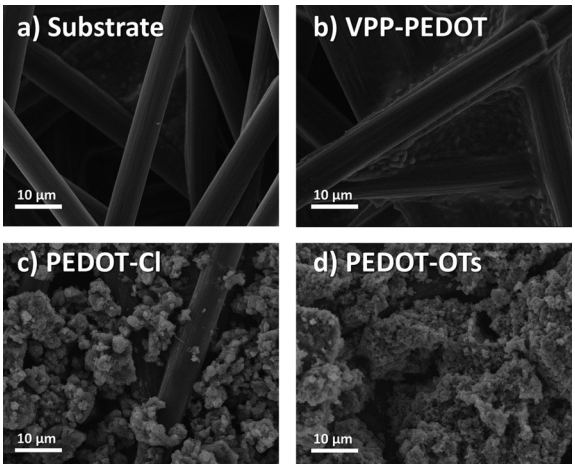

Figure 1. SEM micrographs of a) the bare carbon paper substrate and b–d) the carbon paper substrate coated with PEDOT.

VPP-PEDOT exhibited a different morphology (Figure 1b), in which the individual fibers of the substrate were coated with a smoother coating throughout the bulk of the electrode. This type of coverage originates from the VPP process, in which the initial deposition of the oxidant solution penetrates the fibrous carbon paper through capillary action along/between the carbon fibers.[24] With the current method, however, the amount of VPP-PEDOT on the substrate (0.25 mg cm^{-2}) was only approximately 20% of the loading achieved for PEDOT-Cl and PEDOT-OTs, although this amount could likely be in-

creased considerably by the application of additional VPP-PEDOT layers. Despite the lower mass loading, the VPP-PEDOT has sufficient activity to generate workable capacitors, as will be shown later.

Three-electrode electrochemical characterization

Cyclic voltammograms (CVs) of the different PEDOT materials in emim dca are shown in Figure 2 along with the doping onset potential (DOP) and open-circuit potential (OCP) after synthesis and coating. The different PEDOT materials exhibit similar CVs that are typical of the doping/dedoping process[23b,c,25] with a sharp current increase at the DOP and a small peak followed by a capacitive response above the DOP until the onset of overoxidation at high potentials (Figure S1).

For PEDOT-Cl, the initial current peak intensity decreases and the total charge increases. PEDOT-OTs and VPP-PEDOT also experience a decrease of the peak intensity, but unlike PEDOT-Cl, the total charge in the CV decreases slightly with cycling. The DOP of PEDOT-OTs decreases somewhat with cycling, and this effect is also present to a much smaller degree for PEDOT-Cl and VPP-PEDOT. The overoxidation process becomes evident in the CV above 0.2 V versus ferrocene/ferrocenium ($Fc^{0/+}$; Figure S1), and the onset potential for this process increases with each CV scan as the overoxidized film loses conductivity. This effect is present for all of the PEDOT materials, but the overoxidation process also leads to a greatly increased DOP and decreased doping currents for PEDOT-Cl and PEDOT-OTs. For VPP-PEDOT, the DOP and doping currents are rather stable despite repeated cycling to the overoxidation region, which exemplifies an enhanced stability for VPP-PEDOT in emim dca, and only if the material is cycled above 0.5 V versus $Fc^{0/+}$ does the polymer eventually become totally electrochemically inactive (although the polymer does not detach from the substrate) and the CV charge decreases rapidly.

PEDOT/emim dca coin cells

Symmetric capacitor cells that consist of two PEDOT-coated carbon paper electrodes and emim dca electrolyte were studied to evaluate the device performance. Coin cells with uncoated carbon paper electrodes were also assembled to determine the capacitance of the substrate, which leads to a background specific charge, energy, and capacitance that do not originate from the PEDOT. The carbon paper used for the PEDOT-Cl and PEDOT-OTs electrodes exhibited a very low capacitance ($<1\%$ of the PEDOT cell capacitance; Figure S2), whereas the poly(tetrafluoroethylene) (PTFE) coated carbon paper used for VPP-PEDOT electrodes had a higher capacitance, which gave rise to approximately 22% of the total charge for the VPP-PEDOT cells. The specific capacitance, charge, and energy values for the carbon paper cells at the corresponding currents were subtracted to remove this contribution from the results to allow a better comparison.

Capacitor cell cycling performance

Cycling the PEDOT-Cl and PEDOT-OTs cells at a constant current reveals that they are charged and discharged in a capacitive manner and have a constant capacitance up to approximately 1.1 V cell potential (Figure 3). Above this value the negative electrode is completely dedoped and decreases rapidly in potential if the capacitance is lost, which leads to a rapidly increasing cell potential above 1.1 V (Figure S3). Further charging eventually leads to degradation (most likely at the positive electrode[21]) evident as a potential plateau above 2.1 V, which consumes charge irreversibly that is not recovered upon discharge (Figure S3). However, VPP-PEDOT cells were charged and discharged reversibly from 0 to 2.0 V (Figure 3, see inset for charging to lower cell potentials). Additionally, charging

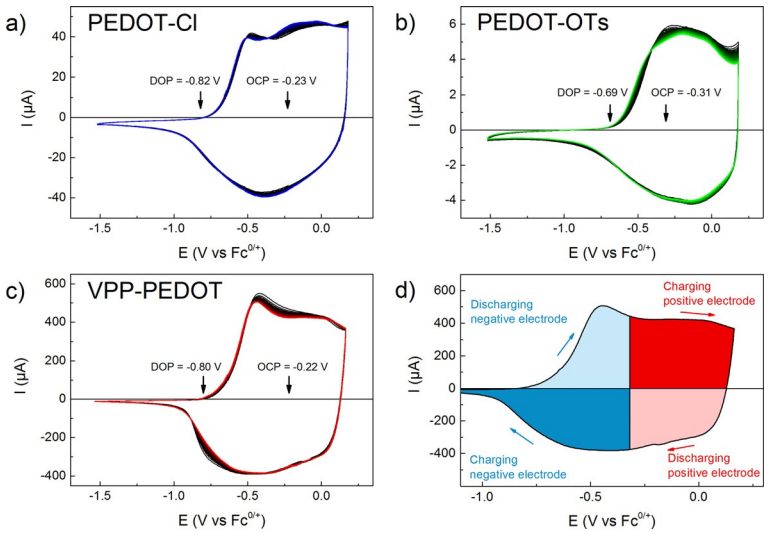

Figure 2. CVs of a) PEDOT-Cl, b) PEDOT-OTs, and c) VPP-PEDOT deposited on glassy carbon in emim dca at 0.1 $V s^{-1}$. 50 scans are shown, of which the first scan is in black and subsequent scans are in a lighter color. d) 50th CV scan of VPP-PEDOT, which shows the charge available for charge (dark colors) and discharge (light colors) of the electrodes in a cell.

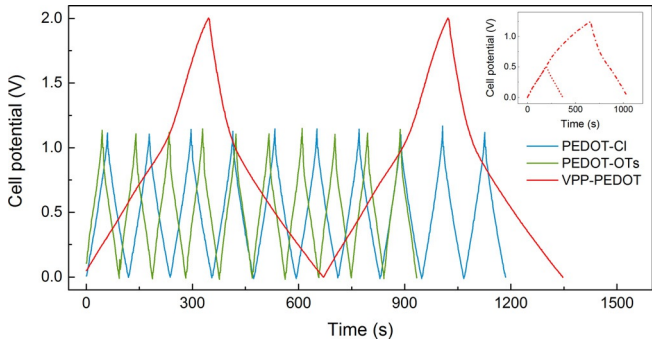

Figure 3. Charge–discharge curves for PEDOT-Cl (blue), PEDOT-OTs (green), and VPP-PEDOT (red) cells at 0.5 A g^{-1} and inset for VPP-PEDOT up to 0.5 and 1.24 V cell potential at 0.8 A g^{-1}.

curves to higher potentials, 0–2.4 V cell potential, that is, above the safe limits, at 1.0 A g^{-1} are shown in Figure S3.

Values of specific capacitance, charge, and energy are summarized in Table 1 for both the coin cell and three-electrode measurements. Specific cell charge and energy at different current densities are shown in Figure 4, and specific cell capacitances are presented in Figure S4. Specific charge and energy values for PEDOT-Cl and PEDOT-OTs are typical of PEDOT[1c,23b] and decrease only slightly with current up to approximately 5 A g^{-1}. VPP-PEDOT exhibits much higher values up to approximately 15 A g^{-1}. At higher current densities, the increased resistance in the cells limits the stored charge. The Coulombic efficiency is close to 100% except at very low current densities (< 50 mA g^{-1}, not shown), below which the reversibility deteriorates as a result of the long times at which the positive electrode is held at a high potential, which leads to degradation reactions.[21]

The doping level of the positive electrode at 1.1 V cell potential was calculated (see Supporting Information for details), and the results are summarized in Table 1.

Stability during cycling and self-discharge

The cycling stability of the cells was investigated by monitoring the capacity fading over several thousand cycles (Figure 5). After an initial decrease in capacity, the cells exhibited rather constant capacities at 65–90% of the initial values. The Coulombic efficiency was consistently 100% for the PEDOT-Cl and PEDOT-OTs cells (within the measurement error) and somewhat lower (> 95%) for the VPP-PEDOT cells because of the cycling above 1.1 V at which not all capacitive charge is regained during discharge (Figure 3). To identify any morphological changes of the polymers during cycling, some electrodes were examined by using SEM after extended cycling (after the electrodes were washed with ethanol to remove the ionic liquid; Figure S5).

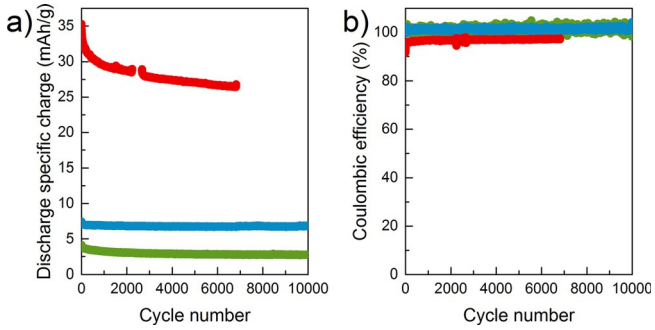

Figure 5. Cycling stability curves that show a) discharge capacity and b) Coulombic efficiency during cycling. PEDOT-Cl (blue), PEDOT-OTs (green), and VPP-PEDOT (red). The VPP-PEDOT cell exhibited some fluctuating behavior after 2000 cycles (not shown in Figure 5a).

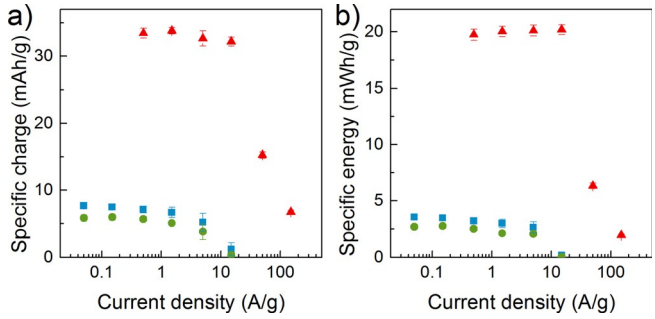

Figure 4. Specific cell a) charge and b) energy for PEDOT cells at varying current densities. Blue squares: PEDOT-Cl, mean of four cells; green circles: PEDOT-OTs, mean of five cells; red triangles: VPP-PEDOT, mean of three cells. Error bars show ± one standard deviation.

Cells charged to 1.1 V (or 2.0 V for VPP-PEDOT) that were allowed to self-discharge over time lost their potential rapidly (Figure 6). A very quick initial potential decrease is followed by a slower but continued decrease that tends to zero cell potential for all cells. The initial potential decrease is especially fast for VPP-PEDOT to reach 1.0 V (half the initial cell potential) in

Table 1. Specific discharge capacitance, charge, and energy of cells at 0.5 A g^{-1} and specific capacitance and charge for electrodes at 1 A g^{-1}. The capacitance values for VPP-PEDOT correspond to the low cell potential region (0–0.8 V). All values are corrected to remove the contribution from the carbon paper substrate.

Polymer	Max. doping level	Cell values						Electrode values			
		specific capacitance		specific charge		specific energy		specific capacitance		specific charge	
		[F g^{-1}]	[mF cm^{-2}]	[mAh g^{-1}]	[μAh cm^{-2}]	[Wh kg^{-1}]	[μWh cm^{-2}]	[F g^{-1}]	[mF cm^{-2}]	[mAh g^{-1}]	[μAh cm^{-2}]
PEDOT-Cl	0.15	23.2	85.0	7.1	26.0	3.2	11.7	92.8	170.0	28.4	52.0
PEDOT-OTs	0.13	18.6	69.4	5.7	21.2	2.5	9.3	74.4	138.8	22.8	42.4
VPP-PEDOT	0.69	76.4	53.2	33.4	16.8	19.8	9.9	305.6	106.4	133.6	33.6

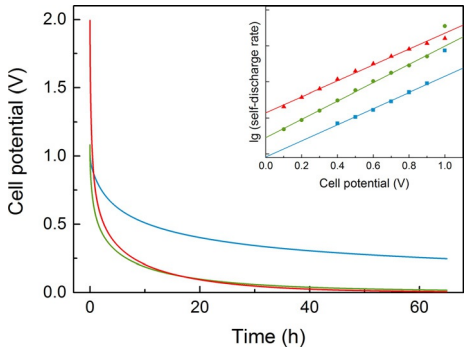

Figure 6. Self-discharge of PEDOT-Cl (blue), PEDOT-OTs (green), and VPP-PEDOT (red) cells. Inset shows the self-discharge rate on a relative logarithmic scale versus cell potential: the self-discharge rate is defined as the rate of charge loss per unit time at certain cell potential values (see Supporting Information). The *y* scale in the inset indicates decades.

0.5 h, and the self-discharge is then similar to that of PEDOT-OTs. For PEDOT-Cl and PEDOT-OTs, half of the cell potential (0.55 V) is reached in 7.8 h and 1.1 h, respectively (for comparison, VPP-PEDOT discharges from 1.1 to 0.55 V in 1.7 h). PEDOT-Cl exhibits a slower self-discharge than the other types, so that after 48 h, when both PEDOT-OTs and VPP-PEDOT are at 0.0 V, PEDOT-Cl still retains 25% of its initial potential (i.e., 0.28 V).

Impedance

Impedance spectra were recorded at zero cell potential for the PEDOT cells (Figure 7) as well as for cells that contain only the carbon paper substrate (Figure S6). All PEDOT cells showed a semicircle response at high frequencies if the data were presented in Nyquist plots (Figure 7), and a diffusion-limited behavior (45° slope) at intermediate frequencies, which transforms into a blocking response (finite length diffusion) at the lowest frequencies, evident as a sharp increase in the absolute value of *Z*''. The onset frequency for the blocking response was

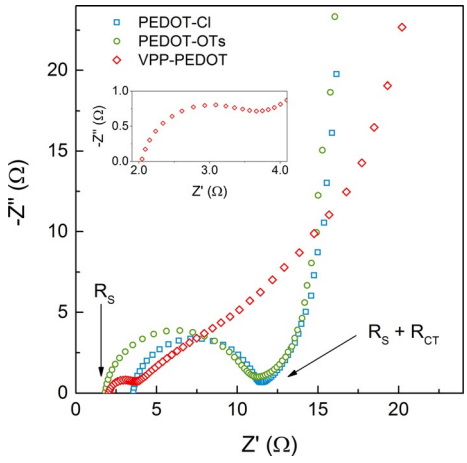

Figure 7. Nyquist plots of PEDOT-Cl (blue), PEDOT-OTs (green), and VPP-PEDOT (red) supercapacitor cells at zero cell potential. The inset shows an enlargement of the VPP-PEDOT. The solution resistance (R_s) and charge-transfer resistance (R_{CT}) are indicated.

lower for the VPP-PEDOT cells than the other cells, indicative of a lower diffusion coefficient in this type of device.[26]

Discussion

PEDOT synthesis and electrode casting

Typically, the polymerization of 3,4-ethylenedioxythiophene (EDOT) from a liquid solution produces porous polymer films,[23b,27] as evidenced by using SEM in this case (Figure 1), which may benefit the cycling performance by improving ion transport through the film. Different oxidants were used for the polymerization of PEDOT-OTs and PEDOT-Cl: $Fe(OTs)\cdot 6H_2O$ and $FeCl_3$, respectively. A substantial concentration of water is present in the PEDOT-OTs reaction mixture (0.36 M, 0.78% m/m), which originates from the oxidant and is known to impede the thiophene polymerization reaction and lead to short polymer chains.[1a] Therefore, shorter polymer segments are expected for PEDOT-OTs in comparison with the other polymers.

In contrast, the VPP process allows a greater control over the kinetics by slowing the polymerization rate without impeding the chain length. The condensation of EDOT monomer onto the liquid oxidant film, the diffusion of "fresh" oxidant to the liquid–vapor interface, and the presence of a triblock copolymer coordinated with the Fe^{3+} yield thin films of PEDOT that have well-ordered and strongly interconnected polymer grains.[16a,28] As the carbon paper substrate is rather brittle, a PTFE-coated carbon paper was used as a substrate for VPP-PEDOT. Although PTFE is not electronically conducting, this layer is sufficiently porous that it does not contribute significantly to the cell resistance (Figure 7). PTFE-coated carbon paper was not used for PEDOT-Cl and PEDOT-OTs because of the difficulties to apply a coating to this substrate.

Three-electrode electrochemical characterization

The three-electrode CVs are similar for the different PEDOT types with DOP values of −0.7 to −0.8 V versus $Fc^{0/+}$, OCP values of −0.2 to −0.3 V versus $Fc^{0/+}$, and overoxidation currents above +0.2 V versus $Fc^{0/+}$ (Figure 2). There are, however, some modest differences between the different polymers: PEDOT-Cl and VPP-PEDOT exhibit a sharp initial peak followed by a broad one. Similar CVs in the ionic liquid 1-ethyl-3-methylimidazolium bis(trifluoromethylsulfonyl)imide have been reported previously for electrochemically polymerized PEDOT.[29] However, PEDOT-OTs has a broader initial peak and slightly decreasing currents at higher potentials.

The CVs change shape upon cycling, in different manners for the different PEDOT types, and this shift is the result of the electrochemical cycling and not because of the contact between the polymer and the ionic liquid as the PEDOT-coated working electrodes were allowed to rest in contact with the ionic liquid for 3 h before the electrochemical characterization. These shifts are because of the changes that occur in the polymer structure as it swells and shrinks repeatedly in the electrolyte and exchanges its initial dopant ions (Cl^- or OTs^-) for dicyanamide.[27]

PEDOT/emim dca coin cells

The performance of symmetric capacitor cells was investigated, that is, with identical PEDOT electrodes that act as the anode and cathode. The symmetric nature of the cells means that in the completely discharged state the cell potential is zero, and in practice all charge cannot be utilized in most applications because the potential is too low. However, in future either electrode can be exchanged readily with, for example, metals[1h,6b] or redox polymers[30] to form hybrid capacitor cells, which can improve the cell potential greatly, and the knowledge obtained from the study of symmetric cells will be valuable for such investigations.

Capacitor cell cycling performance

PEDOT-Cl and PEDOT-OTs capacitor cells exhibited linear $E(t)$ charge and discharge curves to 1.1 V at a constant current of 0.5 A g^{-1} (Figure 3) with specific capacitance values typical of PEDOT ($Q_{spec,cell} \approx 20$ F g^{-1}, $Q_{spec,electrode} \approx 80$ F g^{-1}; Table 1).[1c,23b,31] Above 1.1 V cell potential, the cell capacitance is lost because of the complete reduction of the negative electrode, which thus acts as a self-protection mechanism for the cell to prevent the positive electrode from reaching degrading potentials.[22]

VPP-PEDOT capacitor cells can also be charged and discharged linearly at constant current (Figure 3) up to 0.5, 1.24, and 2.0 V cell potential with significant charge gain, whereas degradation occurs above 2.0 V, in a similar manner to that of PEDOT-Cl and PEDOT-OTs. Furthermore, a much higher capacitance for the VPP-PEDOT than the liquid-phase polymerized PEDOTs was obtained ($Q_{spec,cell} \approx 77$ F g^{-1}, $Q_{spec,electrode} \approx 360$ F g^{-1}; Table 1), which is the highest value reported for neat PEDOT. Unlike the PEDOT-Cl and PEDOT-OTs cells, the VPP-PEDOT cells have some capacitance above 1.1 V cell potential. The PEDOT on the negative electrode is completely dedoped at that cell potential and loses capacitance, but the carbon paper substrate used for the VPP-PEDOT cells has sufficient capacitance to allow slightly more utilization of the positive electrode before degradation occurs above 2.0 V cell potential.

An enhancement in capacitance can be realized only if the interaction between charges, which is commonly taken as the origin of the capacitive response of conducting polymers, is suppressed. An increased distance between charged polymer segments or an improved shielding of charges in the material will lead to a decreased interaction between charges, and would account for the increased capacitance of VPP-PEDOT. It is known that ionic liquids have an extremely high ionic strength that could facilitate the efficient shielding of the bipolaron charges in the PEDOT. However, the same ionic liquid is used for PEDOT-Cl and PEDOT-OTs that do not display enhanced doping levels or specific capacitance values. Therefore, the ionic liquid alone cannot be the source of shielding bipolaron charges. However, the VPP-PEDOT used herein contains a triblock copolymer (Scheme S1) with both ether and siloxane groups that can coordinate to the bipolaron charges. We speculate that the presence of the copolymer adds a significant proportion of ionic conductivity to the VPP-PEDOT electrode and it enables the shielding of like charges that allows the extremely high doping levels. However, we cannot at this point exclude chemical and morphological structural differences inherent from the polymerization conditions (VPP vs. liquid-phase polymerization) as the origin of the increased capacitance.

The maximum doping levels for PEDOT-Cl and PEDOT-OTs (0.15 and 0.13, respectively; Table 1) are in line with doping levels obtained commonly of one charge per 6–8 monomer units. Higher doping levels could be achievable on the positive electrode of the PEDOT-Cl and PEDOT-OTs capacitor cells, although the CVs reveal that overoxidation will limit further doping at higher potentials (Figure S1). Although doping levels up to 0.25–0.33 (one charge per 3–4 monomer units) are sometimes quoted in the literature, this invariably requires high potentials and leads to poor stability.[1a,27] In stark contrast, VPP-PEDOT reaches much higher doping levels, that is, 0.69 charges per monomer at 1.1 V, which is unusually high.[2a,27,31c] As this high doping level is attained without an increase of the potential window it is not merely an effect of an improved resilience towards overoxidation but rather an effect of the increased capacitance of the VPP-PEDOT material. Established differences such as a longer conjugation length and a more linear chain of VPP-PEDOT[28,32] cannot explain the capacitance increase as, at a doping level of 0.69, each bipolaron occupies only approximately three monomer units, and any structural feature that promotes longer conjugation and communication between bipolarons will not stabilize such localized bipolarons. We would hence categorize both the PEDOT and the copolymer to be active materials within the capacitor.

The reactions that occur in the cells during two-electrode constant current cycling (CCC) experiments can be understood by examining the three-electrode CVs (Figure 2). Both electrodes in the cells are originally at OCP, and during the first charging step the negative electrode is dedoped completely (dark blue area in Figure 2 d) and the positive electrode is doped to twice the initial doping level (dark red area in Figure 2 d). If the negative electrode loses capacitance, that potential will decrease quickly until degradation occurs on either electrode. Upon discharge, the charge marked in light blue and light red in Figure 2 d can be withdrawn from the cell. The OCP has a large influence on the available charge, the maximum doping level, and on which electrode will be limiting. For all cells here, the OCP is sufficiently low that the negative electrode is the limiting one.

A comparison of the specific energy and power in a so-called Ragone plot is useful to evaluate device performance. The average specific power during discharge (at the maximum current density with negligible resistance loss) versus specific energy is shown in Figure 8 for capacitors, supercapacitors, and batteries. The performance of the PEDOT cells is also compared to typical electrochemical capacitors as well as state-of-the-art conducting polymer capacitors.[2a] PEDOT-Cl and PEDOT-OTs have similar specific energy and power values as PEDOT cells reported previously,[2a,33] which typically have a lower specific energy than polypyrrole and polyaniline cells.[2a] However, VPP-PEDOT has a significantly better per-

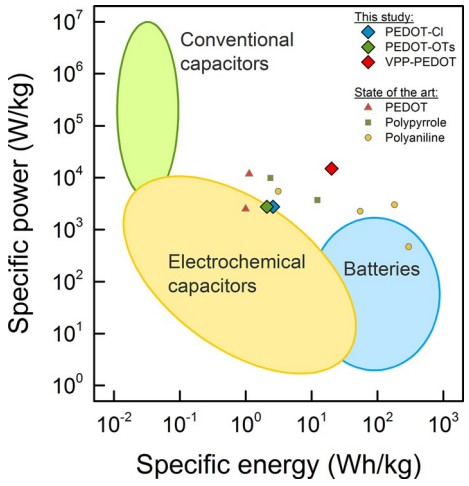

Figure 8. Ragone plot that shows the typical specific power and energy values for conventional capacitors, electrochemical capacitors ("supercapacitors"), and batteries,[2b,3,34] as well as "state-of-the-art" values for symmetric supercapacitors with polypyrrole, polyaniline, or PEDOT.[2a] The PEDOT cells reported in this study are shown as larger diamonds (average power during discharge at 5 A g^{-1} (PEDOT-Cl and PEDOT-OTs) or 15 A g^{-1} (VPP-PEDOT)). Note the logarithmic scales.

formance. In addition to the much greater specific energy, the higher possible current density (Figure 4) leads to an increase in specific power, comparable to that of the best conducting polymer capacitors.

This shows the great potential of the employed ionic liquid, emim dca, as it actually allows faster cycling than that observed commonly in molecular solvents. There is generally a trade-off between specific energy and power in energy-storage devices (Figure 4b), and for the specific energy of the VPP-PEDOT cells, they have a significantly higher specific power than devices reported previously, and vice versa. The VPP-PEDOT cells combine the high specific power of conventional (pure) capacitors with the high specific energy of batteries, a highly sought-after target in energy storage.[2–3,34]

Stability during cycling and self-discharge

PEDOT-Cl and PEDOT-OTs cells have a rather stable specific charge for over 10000 cycles with a specific charge of 2.8 and 6.8 mA h g^{-1} at 1.1 V, respectively, and only experience slight charge decay, which indicates a low rate of degradation during cycling (Figure 5a). VPP-PEDOT cells were cycled to a higher cell potential (2.0 V) than the other polymers, which increased the degradation rate.[21]

Electrodes examined by using SEM after cycling displayed no change in morphology in the dry state (Figure S5). The fact that the electrodes required a few hours of soaking in the electrolyte indicates that the process of taking up electrolyte requires some structural changes as the polymers swell.[27] An investigation of changes in the chemical structure by using spectroscopic methods would be valuable to obtain a more complete picture of the cycling stability in these materials. However, as the ion exchange that takes place between PEDOT and emim dca during cycling will obscure any other spectral variations that might occur, it would be difficult to reliably identify any such structural changes, and it is thus deemed outside the scope of the current study.

During the initial cycling procedure, several processes occur such as ion exchange from the Cl^- or OTs^- dopant ions present from the polymerization to dicyanamide ions that are in vast excess in the system. In the case of PEDOT-Cl, chloride ions will thus be released during cycling, which could possibly lead to the corrosion of the stainless-steel current collectors during long-term operation. We estimate that the chloride concentration in the cells will be in the order of 100–1000 ppm, which is not negligible in this respect. Nevertheless, no negative effect is observed if we compare PEDOT-Cl to PEDOT-OTs (Figure 4, Table 1), and the former even has a superior cycling stability and self-discharge performance (Figures 5 and 6).

The self-discharge of the cells is very rapid, which is usually encountered for conducting polymers (Figure 6).[21,31a] The rate of charge loss during the self-discharge experiment is exponential with potential, as can be seen in the log(rate) versus E_{cell} plots (Figure 6, inset), which are linear below 0.9 V (see details in the Supporting Information). This indicates that a Faradaic reaction that occurs on the positive electrode is responsible for the self-discharge.[21,35] Although the absolute rates are different for the different PEDOT materials, the potential dependence is very similar, which suggests that the process is the same in all cases. The difference in absolute rates might originate from the variation in the solvent-accessible surface area of the different PEDOT types, as the thin-layer VPP-PEDOT has more access to solvent (Figure 1), which makes faster diffusion possible and facilitates self-discharge. PEDOT-Cl has the lowest self-discharge rate, and even though the cell potential is halved within hours, PEDOT-Cl cells can retain a lower potential for some time (Figure 6), which can be utilized if high potentials are not needed or if hybrid cells are employed. The rapid self-discharge of VPP-PEDOT from 2.0 to 1.1 V is because the negative electrode increases in potential in the dedoped state with a very low capacitance. Below this cell potential, the self-discharge is similar to that of PEDOT-OTs despite a significantly higher doping level in VPP-PEDOT, which suggests that the rate of self-discharge is independent of the doping level.

Notably, rapid self-discharge occurs despite the absence of a nucleophilic solvent, which is often implicated as the source of self-discharge.[21,36] This is in line with our recent investigation of self-discharge in polypyrrole, which suggests that the origin of self-discharge in conducting polymers is an intrinsic degradation process on the positive electrode that occurs at appreciable rates even at modest potentials.[21]

Impedance

The Nyquist plots of the PEDOT-based supercapacitor cells (Figure 7) show a semicircle at high frequencies caused by kinetic control at the electrode surface and a 45° line that transforms into a vertical line, which demonstrates a diffusion-limited response towards a blocking electrode.[26] The high-frequency intercept with the Z' axis provides quantitative information on the effective internal resistance caused by the un-

compensated solution resistance (R_s). The same ionic liquid electrolyte was used in all supercapacitor cells, which leads to a similar solution resistance ($R_s \approx 3\ \Omega$). The semicircle radius corresponds to the charge-transfer resistance (R_{CT}), and very similar impedance responses are obtained for the PEDOT-Cl and PEDOT-OTs cells in terms of semicircle radius ($R_{CT} \approx 10\ \Omega$) and diffusion limitations. However, the VPP-PEDOT cell presents a much smaller semicircle ($R_{CT} \approx 2\ \Omega$), which indicates fast electron transfer at the PEDOT interface as a consequence of a lower charge-transfer resistance. The higher doping level of the VPP-PEDOT (i.e., 0.69) corroborates the higher conductivity of VPP-PEDOT. However, the fact that the blocking behavior starts at much lower frequencies for VPP-PEDOT indicates that the ion diffusion is slower in this material (as the VPP-PEDOT layers are not thicker than those of the other PEDOT types, which can be seen by using SEM; Figure 1), possibly because of a more compact structure, compared to the very porous liquid-phase polymerized PEDOT-Cl and PEDOT-OTs. We refrain from extracting quantitative values of the diffusion coefficients as this requires fitting to an equivalent circuit with known reliable values of the constant phase element that represents the capacitive behavior of the cell and its frequency dependence caused by deviations from a perfectly flat surface. We have judged such circuit fitting procedures to be outside the scope of this work.

Conclusions

The main problem with the use of conducting polymers as the active charge-carrying component in energy-storage devices is insufficient specific capacity at stable potentials.[1i,20,21] Reports of higher specific capacities usually involve an increase of the potential window, which drastically decreases the stability of the material.[1i,2a] To achieve high capacity and high cycling stability simultaneously, high capacitance is needed so that more charge can be stored at safe potentials. In this paper we demonstrate a vapor-phase polymerized (VPP) poly(3,4-ethylenedioxythiophene) PEDOT with a high specific capacitance in an ionic liquid electrolyte, which leads to a high specific capacity (306 $F\,g^{-1}$) at doping levels as high as 0.7. Compared to cells based on PEDOT polymerized from liquid solutions that feature a typical PEDOT performance, the specific capacity of the VPP-PEDOT cells is approximately four times as high (e.g., 77 $F\,g^{-1}$). We also show that symmetric supercapacitor cells that feature these materials exhibit extremely high specific capacitance, capacity, and energy and maintain a high specific power as well as a good cycle life. However, the self-discharge that is common for conducting polymers is still an issue in these cells and originates from a Faradaic reaction that involves PEDOT at the positive electrode. We speculate that the efficient shielding of the PEDOT bipolaron charges is the reason for the increased capacitance and we foresee that this strategy could be employed successfully to increase the performance of all conducting polymers in organic energy-storage devices.

Experimental Section

The ionic liquid emim dca (Merck, 99%) was purified by mixing with dichloromethane (1:1 v/v), and the resulting suspension was filtered through a Teflon syringe filter (0.20 μm). The dichloromethane was evaporated, and the ionic liquid was dried under vacuum for 10 h and then stored in a glove box (water content below 47 ppm, as measured by Karl–Fischer titration (Metrohm KF 831)). The 2000 $g\,mol^{-1}$ triblock copolymer poly(ethylene glycol)-poly(dimethylsiloxane)-poly(ethylene glycol) (DBE-U22; Scheme S1) was purchased from Gelest and used without further purification. A 40% m/m solution of iron *p*-toluenesulfonate in *n*-butanol (CB-40) was purchased from Heraeus. EDOT monomer was purchased either from Heraeus or Sigma Aldrich. All other reagents were purchased from Sigma Aldrich and were used without further purification. Carbon paper (AVCarb MGL190) was supplied by Fuel cell Earth (USA) or Shanghai Hesen Electric and was cut into circular disks (∅ = 7.94 mm = 5/16″). SEM images were recorded by using a JEOL Neoscope JCM-5000 (10 kV accelerating voltage).

Synthesis of PEDOT-Cl

PEDOT-Cl was synthesized by the oxidation of EDOT with $FeCl_3$. An acetonitrile (MeCN) solution of EDOT (50 mM) and $FeCl_3$ (200 mM, 4 equiv.) was stirred at RT for 4 h. The formed precipitate was collected by filtration, washed with MeCN and H_2O, and then dried under vacuum for 12 h. Dark blue/black powder was obtained.

PEDOT-Cl (49.2 mg, 95%) and polyvinylidenedifluoride (PVDF; 2.7 mg, 5%) were ground together and mixed with *N*-methylpyrrolidone (NMP; 0.5 g, 0.49 mL). Carbon paper disks were placed on a filter paper and coated with the PEDOT suspension (20 μL). The electrodes were allowed to dry in a fume hood for 5 h and then dried at 100 °C for 12 h.

Synthesis of PEDOT-OTs

PEDOT-OTs was synthesized by the oxidation of EDOT with $Fe(OTs)_3$. An MeCN solution of EDOT (15 mM) and $Fe(OTs)_3{\cdot}6H_2O$ (60 mM, 4 equiv.) was stirred at RT for 70 h. The formed precipitate was collected by filtration, washed with MeCN, and then dried at 100 °C for 12 h. Dark blue/black powder was obtained.

PEDOT-OTs (47.1 mg, 95%) and PVDF (2.1 mg, 5%) were ground together and mixed with NMP (0.5 g, 0.49 mL). Carbon paper disks were placed on a filter paper and coated with the PEDOT suspension (2 × 20 μL). The electrodes were allowed to dry in a fume hood for 5 h and then dried at 100 °C for 12 h.

Synthesis of VPP-PEDOT

PEDOT doped with OTs^- was also synthesized by the oxidation of EDOT with $Fe(OTs)_3$ using the VPP process (VPP-PEDOT). In this process, the oxidant solution contained DBE-U22 triblock copolymer (1.5 g; Scheme S1), CB-40 solution (2 g), and ethanol (3 g). Four PEDOT layers were deposited on PTFE-coated carbon paper (loading 0.25 $mg\,cm^{-2}$) by repeating the vacuum VPP of the EDOT monomer (50 min) following the general method described elsewhere.[16a,32] After each VPP cycle, the electrodes were soaked and washed in ethanol to remove any excess oxidant and dried at 40 °C.

VPP-PEDOT-coated carbon paper disks were dried at 100 °C for 12 h before coin cell assembly.

Electrochemical measurements

A Biologic VMP3/Z multi-channel potentiostat was used for all three-electrode electrochemical measurements. A glassy carbon disk working electrode (ALS Co. Ltd., Japan, $\varnothing = 1$ mm) was coated with 200 nL of the corresponding PEDOT/PVDF suspension, dried in a fume hood for 12 h and then at 70 °C for 1 h. A Pt wire was used as the counter electrode, and the reference electrode consisted of a Ag wire immersed in emim dca that contained 5 mM silver trifluoromethanesulfonate (−0.52 V vs. the ferrocene redox couple; $Fc^{0/+}$). The working electrodes were allowed to rest in the electrolyte for 3 h inside a glove box before characterization, and the OCP was measured before characterization by CV. The DOP was defined as the lowest potential with 1% of the oxidation peak current in the CV after the subtraction of a linear baseline extrapolated from the nondoped region. The electrolyte was kept under a N_2 atmosphere throughout the measurements, which were performed outside the glove box, and the water content was at most 1.7% after the three-electrode experiments. All measurements were performed at RT (21 °C).

Coin cells (Hohsen, 2032) were constructed in an Ar-filled glovebox using two carbon paper electrodes to sandwich a glass fiber separator (Advantec GA55, 0.21 mm thickness, 14.3 mm diameter) soaked in emim dca. A 1.4 mm spring and 1.0 mm spacer was used (see our previous publication for further details on the coin cells[6b]). The cells were sealed and then allowed to rest for at least 3 h before use. The cells were then characterized outside the glovebox at RT (21 °C) by using either a Neware battery tester or a Biologic VMP3/Z multichannel potentiostat. All cells were subjected to the following series of experiments: 1) preconditioning CCC at 5 (VPP-PEDOT) or 0.5 $A g^{-1}$ (PEDOT-Cl and PEDOT-OTs) until a stable response was obtained, 2) impedance, 3) CCC at various current densities, and 4) impedance. After these measurements, some cells were subjected to self-discharge experiments or extended CCC to test cycling stability.

CCC at different specific currents (step 3 above) was performed for 10 cycles for each current with 1 min resting time between the different currents. The specific charge of the coin cells was determined as $Q_{spec,cell} = \int j(t)dt$ during the 10th discharge, in which $j(t)$ is the specific current over time. The specific energy was determined as $W_{spec,cell} = \int j(t) \cdot E(t)dt = \int P(t)dt$ during the 10th discharge, in which $E(t)$ and $P(t)$ are the cell potential and specific cell power over time, respectively. The specific capacitance was determined as $C_{spec,cell} = \frac{Q_{spec,cell}}{E(t=0)}$ during the 10th discharge. All specific cell values are normalized with respect to the total mass of PEDOT on both electrodes and corrected for the corresponding value of the carbon paper substrate. Specific cell values are a factor of 0.25 of the corresponding specific electrode values normalized with respect to mass.[3,22] If normalized with respect to area, the corresponding factor is 0.5.[3,22] Doping levels were calculated from $Q_{spec,cell}$ values as detailed in the Supporting Information. As a measure of cycling stability, the specific charge during discharge and coulombic efficiency was recorded until cell failure, and the data were smoothed using a 20 point moving average.

Electrochemical impedance spectroscopy was performed at 0 V cell potential between 100 mHz and 100 kHz with an amplitude of 10 mV. Self-discharge measurements were performed by charging a cell first with a constant current of 0.5 $A g^{-1}$ and then with constant potential until the current dropped below 0.05 $A g^{-1}$. The OCP was then measured over time. The rate of the self-discharge process was then calculated from the $E(t)$ profile and the cell capacitance (see details in the Supporting Information).

Acknowledgements

Funding from the European Union's Horizon 2020 Programme (H2020/2014-2020) under grant agreement n° 644631 (ROLL-OUT), The Olle Byggmästare Foundation, and the Swedish Foundation for Strategic Research is acknowledged. C.P.G., P.C.H., and M.F. acknowledge financial support from the Australian Research Council (ARC) through the ARC Centre of Excellence for Electromaterials Science (ACES). M.F. also gratefully acknowledges funding through the ARC Laureate program.

Keywords: electrochemistry · doping · ionic liquids · polymerization · polymers

[1] a) P. Novák, K. Müller, K. S. V. Santhanam, O. Haas, *Chem. Rev.* **1997**, *97*, 207; b) R. S. Kularatne, H. D. Magurudeniya, P. Sista, M. C. Biewer, M. C. Stefan, *J. Polym. Sci. Part A* **2013**, *51*, 743; c) G. A. Snook, P. Kao, A. S. Best, *J. Power Sources* **2011**, *196*, 1; d) O. Inganäs, *Chem. Soc. Rev.* **2010**, *39*, 2633; e) U. Lange, N. V. Roznyatovskaya, V. M. Mirsky, *Anal. Chim. Acta* **2008**, *614*, 1; f) E. W. H. Jager, E. Smela, O. Inganäs, *Science* **2000**, *290*, 1540; g) C. K. Chiang, *Polymer* **1981**, *22*, 1454; h) D. Naegele, R. Bittihn, *Solid State Ionics* **1988**, *28–30*, 983; i) Z. Song, H. Zhou, *Energy Environ. Sci.* **2013**, *6*, 2280; j) A. Malti, J. Edberg, H. Granberg, Z. U. Khan, J. W. Andreasen, X. Liu, D. Zhao, H. Zhang, Y. Yao, J. W. Brill, I. Engquist, M. Fahlman, L. Wågberg, X. Crispin, M. Berggren, *Adv. Sci.* **2016**, *3*, 1500305.

[2] a) L. Nyholm, G. Nyström, A. Mihranyan, M. Strømme, *Adv. Mater.* **2011**, *23*, 3751; b) H. D. Abruña, Y. Kiya, J. C. Henderson, *Phys. Today* **2008**, *61*, 43.

[3] M. Winter, R. J. Brodd, *Chem. Rev.* **2004**, *104*, 4245.

[4] R. Holze, Y. P. Wu, *Electrochim. Acta* **2014**, *122*, 93.

[5] a) P. Tammela, Z. Wang, S. Frykstrand, P. Zhang, I.-M. Sintorn, L. Nyholm, M. Strømme, *RSC Adv.* **2015**, *5*, 16405; b) N. Vucaj, M. D. J. Quinn, C. Baechler, S. M. Notley, P. Cottis, P. Hojati-Talemi, M. V. Fabretto, G. G. Wallace, P. J. Murphy, D. R. Evans, *Chem. Mater.* **2014**, *26*, 4207; c) S. Lagoutte, P.-H. Aubert, M. Pinault, F. Tran-Van, M. Mayne-L'Hermite, C. Chevrot, *Electrochim. Acta* **2014**, *130*, 754; d) J. M. D'Arcy, M. F. El-Kady, P. P. Khine, L. Zhang, S. H. Lee, N. R. Davis, D. S. Liu, M. T. Yeung, S. Y. Kim, C. L. Turner, A. T. Lech, P. T. Hammond, R. B. Kaner, *ACS Nano* **2014**, *8*, 1500; e) W. Zhou, Y. Yu, H. Chen, F. J. DiSalvo, H. D. Abruña, *J. Am. Chem. Soc.* **2013**, *135*, 16736–16743.

[6] a) C. Karlsson, H. Huang, M. Strømme, A. Gogoll, M. Sjödin, *J. Phys. Chem. C* **2014**, *118*, 23499; b) T. J. Simons, M. Salsamendi, P. C. Howlett, M. Forsyth, D. R. MacFarlane, C. Pozo-Gonzalo, *ChemElectroChem* **2015**, *2*, 2071; c) L. Yang, X. Huang, A. Gogoll, M. Strømme, M. Sjödin, *J. Phys. Chem. C* **2015**, *119*, 18956.

[7] K. Lota, V. Khomenko, E. Frackowiak, *J. Phys. Chem. Solids* **2004**, *65*, 295.

[8] L. Ran, C. Seung Il, L. Sang Bok, *Nanotechnology* **2008**, *19*, 215710.

[9] W. Li, J. Chen, J. Zhao, J. Zhang, J. Zhu, *Mater. Lett.* **2005**, *59*, 800.

[10] J. Jang, J. Bae, E. Park, *Adv. Mater.* **2006**, *18*, 354.

[11] R. Liu, S. I. Cho, S. B. Lee, *Nanotechnology* **2008**, *19*, 215710.

[12] a) O. Bubnova, Z. U. Khan, A. Malti, S. Braun, M. Fahlman, M. Berggren, X. Crispin, *Nat. Mater.* **2011**, *10*, 429; b) O. Bubnova, Z. U. Khan, H. Wang, S. Braun, D. R. Evans, M. Fabretto, P. Hojati-Talemi, D. Dagnelund, J.-B. Arlin, Y. H. Geerts, S. Desbief, D. W. Breiby, J. W. Andreasen, R. Lazzaroni, W. M. Chen, I. Zozoulenko, M. Fahlman, P. J. Murphy, M. Berggren, X. Crispin, *Nat. Mater.* **2014**, *13*, 190.

[13] a) B. Winther-Jensen, O. Winther-Jensen, M. Forsyth, D. R. MacFarlane, *Science* **2008**, *321*, 671; b) P. P. Cottis, D. Evans, M. Fabretto, S. Pering, P. Murphy, P. Hojati-Talemi, *RSC Adv.* **2014**, *4*, 9819.

[14] L. Tong, K. H. Skorenko, A. C. Faucett, S. M. Boyer, J. Liu, J. M. Mativetsky, W. E. Bernier, W. E. Jones Jr., *J. Power Sources* **2015**, *297*, 195.

[15] R. Brooke, M. Fabretto, P. Hojati-Talemi, P. Murphy, D. Evans, *Polymer* **2014**, *55*, 3458.

[16] a) M. V. Fabretto, D. R. Evans, M. Mueller, K. Zuber, P. Hojati-Talemi, R. D. Short, G. G. Wallace, P. J. Murphy, *Chem. Mater.* **2012**, *24*, 3998; b) B.

Winther-Jensen, K. Fraser, C. Ong, M. Forsyth, D. R. MacFarlane, *Adv. Mater.* **2010**, *22*, 1727.
[17] a) D. R. MacFarlane, N. Tachikawa, M. Forsyth, J. M. Pringle, P. C. Howlett, G. D. Elliott, J. H. Davis, M. Watanabe, P. Simon, C. A. Angell, *Energy Environ. Sci.* **2014**, *7*, 232; b) D. R. MacFarlane, M. Forsyth, P. C. Howlett, M. Kar, S. Passerini, J. M. Pringle, H. Ohno, M. Watanabe, F. Yan, W. Zheng, S. Zhang, J. Zhang, *Nat. Rev. Mater.* **2016**, *1*, 15005.
[18] M. Kar, T. J. Simons, M. Forsyth, D. R. MacFarlane, *Phys. Chem. Chem. Phys.* **2014**, *16*, 18658.
[19] T. J. Simons, D. R. MacFarlane, M. Forsyth, P. C. Howlett, *ChemElectroChem* **2014**, *1*, 1688.
[20] Y. Liang, Z. Tao, J. Chen, *Adv. Energy Mater.* **2012**, *2*, 742.
[21] H. Olsson, M. Strømme, L. Nyholm, M. Sjödin, *J. Phys. Chem. C* **2014**, *118*, 29643.
[22] H. Olsson, G. Nyström, M. Strømme, M. Sjödin, L. Nyholm, *Electrochem. Commun.* **2011**, *13*, 869.
[23] a) M. A. Vorotyntsev, D. V. Konev, U. Lange, Y. V. Tolmachev, M. Skompska, *Electrochim. Acta* **2013**, *110*, 452; b) G. P. Pandey, A. C. Rastogi, C. R. Westgate, *J. Power Sources* **2014**, *245*, 857; c) J. M. Pringle, M. Forsyth, D. R. MacFarlane, K. Wagner, S. B. Hall, D. L. Officer, *Polymer* **2005**, *46*, 2047.
[24] E. Lorenceau, T. Senden, D. Quéré in *Molecular Gels* (Eds: R. Weiss, P. Terech), Springer, Netherlands, **2006**, 223.
[25] H. Randriamahazaka, C. Plesse, D. Teyssié, C. Chevrot, *Electrochim. Acta* **2005**, *50*, 4222.
[26] C. Ho, I. D. Raistrick, R. A. Huggins, *J. Electrochem. Soc.* **1980**, *127*, 343.
[27] J. Heinze, B. A. Frontana-Uribe, S. Ludwigs, *Chem. Rev.* **2010**, *110*, 4724.
[28] D. Evans, M. Fabretto, M. Mueller, K. Zuber, R. Short, P. Murphy, *J. Mater. Chem.* **2012**, *22*, 14889.
[29] H. Randriamahazaka, C. Plesse, D. Teyssié, C. Chevrot, *Electrochem. Commun.* **2003**, *5*, 613.
[30] a) C. Karlsson, H. Huang, M. Strømme, A. Gogoll, M. Sjödin, *Electrochim. Acta* **2015**, *179*, 336; b) C. Karlsson, H. Huang, M. Strømme, A. Gogoll, M. Sjödin, *RSC Adv.* **2015**, *5*, 11309; c) L. Yang, V.-A. Mihali, D. Brandell, M. Strømme, M. Sjödin, *J. Phys. Chem. C* **2014**, *118*, 25956; d) B. Häupler, A. Wild, U. S. Schubert, *Adv. Energy Mater.* **2015**, *5*, 1402034; e) T. Janoschka, M. D. Hager, U. S. Schubert, *Adv. Mater.* **2012**, *24*, 6397.
[31] a) A. M. Österholm, D. E. Shen, A. L. Dyer, J. R. Reynolds, *ACS Appl. Mater. Interfaces* **2013**, *5*, 13432; b) G. P. Pandey, A. C. Rastogi, *J. Electrochem. Soc.* **2012**, *159*, A1664; c) J. D. Stenger-Smith, C. K. Webber, N. Anderson, A. P. Chafin, K. Zong, J. R. Reynolds, *J. Electrochem. Soc.* **2002**, *149*, A973.
[32] M. Mueller, M. Fabretto, D. Evans, P. Hojati-Talemi, C. Gruber, P. Murphy, *Polymer* **2012**, *53*, 2146.
[33] a) V. Khomenko, E. Raymundo-Piñero, E. Frackowiak, F. Béguin, *Appl. Phys. A* **2006**, *82*, 567; b) J. C. Carlberg, O. Inganäs, *J. Electrochem. Soc.* **1997**, *144*, L61.
[34] a) M. Armand, J.-M. Tarascon, *Nature* **2008**, *451*, 652; b) P. Simon, Y. Gogotsi, *Nat. Mater.* **2008**, *7*, 845.
[35] B. E. Conway in *Electrochemical Supercapacitors: Scientific Fundamentals and Technological Applications*, Kluwer Academic/Plenum Publishers, New York, **1999**, 562.
[36] F. Beck, P. Braun, M. Oberst, *Ber. Bunsen-Ges.* **1987**, *91*, 967.

Received: March 10, 2016
Revised: May 10, 2016
Published online on June 21, 2016